



Preparation and characterisation of Co–Fe–Ni–M–Si–B (M = Zr, Ti) amorphous powders by wet mechanical alloying



B.V. Neamțu^{a, *}, H.F. Chicinaș^a, T.F. Marinca^a, O. Isnard^{b, c}, I. Chicinaș^a

^a Materials Science and Engineering Department, Technical University of Cluj-Napoca, 103-105, Muncii Avenue, 400641, Cluj-Napoca, Romania

^b Université Grenoble Alpes, Institut NEEL, F-38042, Grenoble, France

^c CNRS, Institut NEEL, 25 rue des martyrs, BP166, F-38042, Grenoble, France

ARTICLE INFO

Article history:

Received 4 January 2016

Received in revised form

22 February 2016

Accepted 29 February 2016

Available online 3 March 2016

Keywords:

Amorphous materials

Magnetic materials

Powder metallurgy

Magnetic properties

Powder diffraction

ABSTRACT

Co-based amorphous alloys were prepared via wet mechanical alloying process starting from elemental powders. The reference alloy $\text{Co}_{70}\text{Fe}_4\text{Ni}_2\text{Si}_{15}\text{B}_9$ (at. %) as well as the alloys derived from this composition by the substitution of 5 at.% of Zr or Ti for Si or B ($\text{Co}_{70}\text{Fe}_4\text{Ni}_2\text{Si}_{15}\text{B}_4\text{Zr}_5$, $\text{Co}_{70}\text{Fe}_4\text{Ni}_2\text{Si}_{15}\text{B}_4\text{Ti}_5$, $\text{Co}_{70}\text{Fe}_4\text{Ni}_2\text{Si}_{10}\text{B}_9\text{Zr}_5$ and $\text{Co}_{70}\text{Fe}_4\text{Ni}_2\text{Si}_{10}\text{B}_9\text{Ti}_5$) are obtained in amorphous state, according to X-ray diffraction (XRD) investigation, after 40 h of milling. The calculated amount of amorphous fraction reaches 99% after 40 h of milling. The largest increase of the crystallisation temperature was induced by the substitution of Zr or Ti for Si while, regardless of the type of substitution, an important increase of the Curie temperature of the alloy was obtained. A Co-based solid solution, with Co_2Si and Co_2B phases, result after crystallisation of the amorphous alloys as proved by XRD investigations. Saturation magnetisation of the alloys decreases upon increasing milling time, however it remains larger than the saturation magnetisation of the reference alloy. This was discussed in correlation with the specificity of the wet mechanical alloying process and the influence of the chemical bonding between Co and metalloids atoms over the magnetic moment of Co.

© 2016 Elsevier B.V. All rights reserved.

1. Introduction

Since 1967, when the first ferromagnetic amorphous material ($\text{Fe}_{80}\text{P}_{13}\text{C}_7$) was developed [1], the amorphous soft magnetic alloys are extensively studied from fundamental and applicative point of view. Besides the Fe–Si grain oriented alloys, the amorphous and nanocrystalline alloys are used more and more as soft magnetic materials for energy conversion. From the lack of long range atomic ordering resides a series of electric and magnetic characteristics, such as lack of the magnetocrystalline anisotropy and high electrical resistivity, which make the amorphous magnetic materials viable candidates for a series of modern applications [2].

There are a series of techniques that are used in order to produce amorphous alloys, the most carried out way to produce such material is rapid quenching [3]. Beside this, mechanosynthesis route has been successfully used to produce amorphous alloys of various compositions in powder form [4]. This technique offers a series of advantages over the rapid quenching such as: relatively low-cost

equipment, simplicity in operation, low-temperature processing, extension of the solubility, synthesis of alloys made from elements with very different melting points, large number of processing parameters that can be set, the capacity to produce large amounts of material, etc. [5,6].

During mechanical alloying (MA), a mixture of elemental powders or pre-alloyed powders is subjected to high energy ball milling process. In the course of the MA process, a large number of defects are induced together with a slight increase of the temperature of the powder and milling bodies (balls and vials). Due to these phenomena, the atomic inter-diffusion takes place, and finally the alloy is formed [7]. In some cases (when materials with high plasticity are processed) it is difficult to achieve a balance between the cold welding and fracturing phenomena (cold welding phenomena being predominant). In such cases, together with the milling bodies and the powders to be milled, a certain quantity (not larger than 5 wt.% of total processed mass powder) of process control agent (PCA) is added [5,6]. The PCAs are, most commonly, organic substances which act as surfactants, reducing the quantity of cold welding processes and leading to the achievement of a balance between cold welding and fracturing phenomena [7].

* Corresponding author.

E-mail address: Bogdan.Neamtu@stm.utcluj.ro (B.V. Neamțu).

The Co-based amorphous alloys present outstanding soft magnetic properties such as low coercivity, high permeability and low hysteresis losses that originate from their near zero magnetostriction and magnetocrystalline anisotropy [2,8]. MA was successfully used to prepare Co-based amorphous powders of several binary, ternary, quaternary and multi-component systems such as: Co–Nb [9], Co–B [10], Co–B–Si [11], Co–Cr–Mo [12], Co–Fe–Si–B [13], Co–Fe–Ta–B [14], Co–Fe–(Zr,Ti)–B [15], Co–Nb–Zr–B [16], etc. Alternatively, mechanosynthesis was proved to be an effective technique to prepare Co-based powders by milling of the amorphous ribbons obtained by rapid quenching technique [17,18].

This study aims to prepare amorphous Co-based alloys via MA and to improve the thermal stability of the amorphous alloys (increase of the crystallisation temperature) by substitution of Si or B for Zr or Ti. The increase of the crystallisation temperature of the amorphous phase is of utmost importance taking into account the subsequent compaction of the powder by a sintering technique (most probably spark plasma sintering).

2. Experimental procedure

The reference alloy $\text{Co}_{70}\text{Fe}_4\text{Ni}_2\text{Si}_{15}\text{B}_9$ (at. %) as well as the alloys derived from the substitution of 5 at.% of Zr or Ti for Si or B ($\text{Co}_{70}\text{Fe}_4\text{Ni}_2\text{Si}_{15}\text{B}_9\text{Zr}_5$, $\text{Co}_{70}\text{Fe}_4\text{Ni}_2\text{Si}_{15}\text{B}_4\text{Ti}_5$, $\text{Co}_{70}\text{Fe}_4\text{Ni}_2\text{Si}_{10}\text{B}_9\text{Zr}_5$ and $\text{Co}_{70}\text{Fe}_4\text{Ni}_2\text{Si}_{10}\text{B}_9\text{Ti}_5$) were prepared by wet MA using a mixture of elemental powders. The composition was chosen to keep a large amount of magnetic 3d elements such as Fe, Co and Ni, whereas additions of p elements such as B or Si are known to favour a larger resistivity. Boron is also often reported to favour the amorphous state of such alloy. Finally, non-magnetic transition metal elements were used to replace part of either Si or B content. The main characteristics of the elemental powders used are: Co (99.8% purity, particle size range 45–150 μm), Fe type NC 100.24 (98.5% purity, particle size <150 μm), Ni type 123-carbonyl (99.8% purity, particle size <7 μm), Si (99.9% purity, particle size <150 μm), amorphous B (amorphous powder, 99.8% purity, particle size <45 μm), Ti (99.5% purity, particle size <150 μm) and Zr (99.2% purity, particle size <45 μm). The starting mixture (denoted as SS) was prepared in a Turbula-type blender for 30 min to ensure a homogenous distribution of elements in the powder. The as-obtained mixture was processed in high energy planetary ball mill (Fritsch Pulverisette 6) using benzene as PCA. Benzene was chosen as PCA due to the relative high stability of its aromatic ring. The samples were milled up to 40 h in identical conditions. The milling bodies (vials and balls) are manufactured from tempered steel. The ball to powder ratio (BPR) was chosen to be 16:1. This led to a filling factor of about 50% of the 500 ml milling vials. The disc rotational speed was set at 350 rpm. Every time sampling was performed, 1 ml of C_6H_6 was added, to prevent the particles cold welding and to counteract the amount of PCA that evaporate. In order to avoid powder oxidation during milling process, argon atmosphere was used. Also, for the same motivation, the sample collection was done in a glove-box installation (Iteco Engineering SGS 30) under Ar atmosphere.

The structural evolution of the alloys was investigated by XRD using the Co $K\alpha$ radiation ($\lambda = 1.7903 \text{ \AA}$) in order to avoid the fluorescence from Co or Fe atoms that are the main constituents of the studied alloys. The equipment that was used is an INEL® Equinox 3000 powder diffractometer functioning in reflection mode. The scanned interval was $2\theta = 20\text{--}110^\circ$. The mean crystallite size was calculated from the full-width-at-half maximum (FWHM) of the diffraction peaks according to Scherrer's formula. In order to do so, the resolution of the diffractometer has been determined from the diffraction pattern of a reference sample [19]. Based on the coherent polycrystalline model [20,21], the amount of amorphous fraction in the material was estimated using the

following formula:

$$f_{gb} = 1 - \frac{(D-d)^3}{D^3}; \quad (1)$$

where, D represents the mean crystallite size and d is the effective thickness of the grain boundary which is about 2–3 atomic layers as suggested in the literature [21,22].

The thermal stability of the alloys has been studied by differential scanning calorimetry (DSC). The scanned temperature range was 20–900 $^\circ\text{C}$, with a heating/cooling rate of 20 $^\circ\text{C}/\text{min}$. All of the measurements were performed on a Setaram Labsys apparatus under high purity Ar atmosphere.

The chemical composition of the samples was investigated by X-rays microanalysis, using a scanning electron microscope type Jeol-JSM 5600 LV equipped with an EDX spectrometer (Oxford Instruments, Inca 200 soft).

The magnetisation measurements ($M(H)$) performed on the samples were done at room temperature using the sample extraction method in a continuous magnetic field up to 10 T. Saturation magnetisation has been derived from the first magnetisation curves, in the high magnetic field region by extrapolation to zero field of the magnetization obtained in the magnetic field higher than 4 T. Also, the Curie temperature of the amorphous powders was determined from the thermomagnetic measurements ($M(T)$), in the temperature range 20–900 $^\circ\text{C}$, with a heating rate of 10 $^\circ\text{C}/\text{min}$. In order to avoid oxidation, the powder was sealed in a quartz tube under vacuum (10^{-3} Torr).

3. Results and discussions

The X-ray diffraction patterns of the reference alloy $\text{Co}_{70}\text{Fe}_4\text{Ni}_2\text{Si}_{15}\text{B}_9$ have been recorded for the samples milled for different durations, up to 40 h and are presented in Fig. 1. Since the XRD patterns exhibit very similar milling time dependence for the five studied compositions, only the evolution of the XRD patterns versus milling time corresponding to the reference samples are presented. In the XRD pattern of the starting sample, referred to as SS, of the $\text{Co}_{70}\text{Fe}_4\text{Ni}_2\text{Si}_{15}\text{B}_9$ reference alloy, one can notice the peaks characteristic of elemental Co (hcp), Co (fcc), Fe, Ni and Si according to JCPDS files no. 89–4308, 15–0806, 06–0696, 04–0850 and 27–1402 respectively. Although not presented here, the XRD

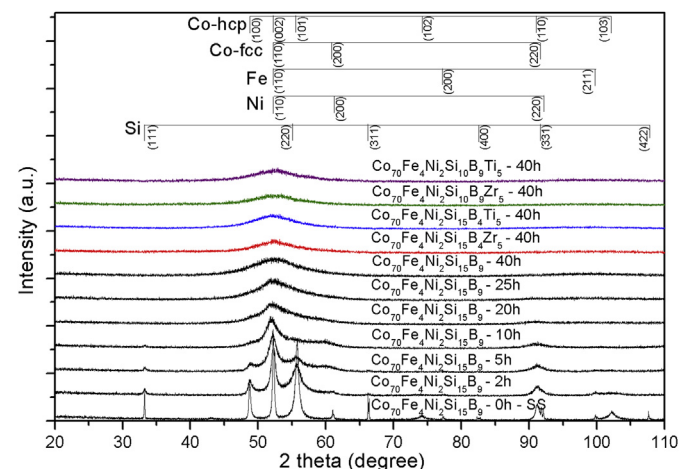


Fig. 1. Evolution of the X-ray diffraction patterns for the $\text{Co}_{70}\text{Fe}_4\text{Ni}_2\text{Si}_{15}\text{B}_9$ (reference alloy) wet milled using benzene for the indicated time up to 40 h. For comparison, the XRD patterns of the substitution alloys milled for 40 h are also presented. ($\lambda = 1.7903 \text{ \AA}$).

investigation of the elemental Co powder used in this study, reveal the presence of the above mentioned crystallographic structures of Co. The co-existence of these two allotropic forms of Co is a usual characteristic at room temperature and is, as discussed elsewhere, favoured by the presence of small amount of impurities or structural defects [22]. The characteristic peaks of boron are not visible due to both its low X-ray scattering factor and amorphous state. Although, not presented here, it worth mentioning that the only difference in the XRD patterns of the starting mixtures corresponding to the substitution alloys is the presence of the Bragg peaks characteristic of Ti or Zr elements.

By increasing the milling time, a broadening of the Bragg reflections and a small shift towards lower angles can be observed in the XRD patterns. The broadening of the peaks is an effect of the inhomogeneous second order internal stresses induced during the MA process. Also, the diminution of the crystallite size induced by milling leads to the broadening of the Bragg reflections. The displacement of the Bragg reflections to smaller angles is a result of first-order internal stresses induced by milling. Similarly, some of the peaks are disappearing, even the peaks characteristic of the hexagonal Co, suggesting the dissolution of the atoms and the formation of a cubic Co-based solid solution (fcc). Increasing milling time up to 10 h is leading to the complete dissolution of the elements. At this point, according to the XRD pattern, the material consists of a single fcc Co-based solid solution. The peak width broadening suggests a small crystallite size, which indicates a larger amount of atoms residing in grain boundaries. It is assumed that the atoms located at the grain boundary are not strictly ordered and consequently part of an amorphous state, therefore the continuous crystallite size diminishing is leading to the increase of the volume occupied by the amorphous phase. The decrease of the crystalline phase is suggested also by the significant broadening of the peak for milling durations higher than 10 h. According to the XRD investigation and considering the experimental limits of this technique the following conclusion can be drawn: the complete amorphisation of the alloy occurs after 40 h of MA. This is suggested by the presence of a single broadened feature on the XRD pattern indicating the absence of long range atomic ordering in the material. Although the XRD pattern corresponding to the sample milled for 25 h reveals also a single broad feature, its asymmetry towards higher angles suggests the presence of a small crystalline/nano-crystalline fraction embedded in an amorphous matrix. In any of the four cases, regardless of the composition or substitution scheme, the complete amorphisation is observed after 40 h of MA. This behaviour suggest at a first glance the fact that the substitution of 5 at. % of Ti or Zr for the same amount of Si or B is not leading to any changes in the powder amorphisation process. A wide range of milling durations are reported in literature for the amorphisation of Co-based alloys obtained from a mixture of elemental powders, depending upon milling equipment and milling parameters. For example, in the case of $\text{Co}_{60}\text{Fe}_5\text{Ni}_5\text{Ti}_{25}\text{B}_5$ (at.%) it was found that 3.5 h of milling are sufficient for the complete amorphisation of the alloy while in the case of $\text{Co}_{40}\text{Fe}_{22}\text{Ta}_8\text{B}_{30}$ (at.%) alloy, the amorphisation was reached after 200 h of milling (the fraction of the amorphous phase reach 96% of the alloy) [14,23].

Fig. 2 presents the milling time dependence of the mean crystallite size and amorphous fraction for the alloy in which 5 at.% of Si or B was replaced with the same amount of Ti or Zr. The values of the mean crystallites size presented in Fig. 2 are underestimated due to the influence of second order internal stresses presented in the samples that are not taken into account. The mean crystallite size was estimated using Scherrer's formula for the Bragg reflection (110) of the fcc Co-based solid solution. One can observe that for the investigated alloys the mean crystallite size has a classic evolution, it decreases upon increasing the milling time and tends to saturate.

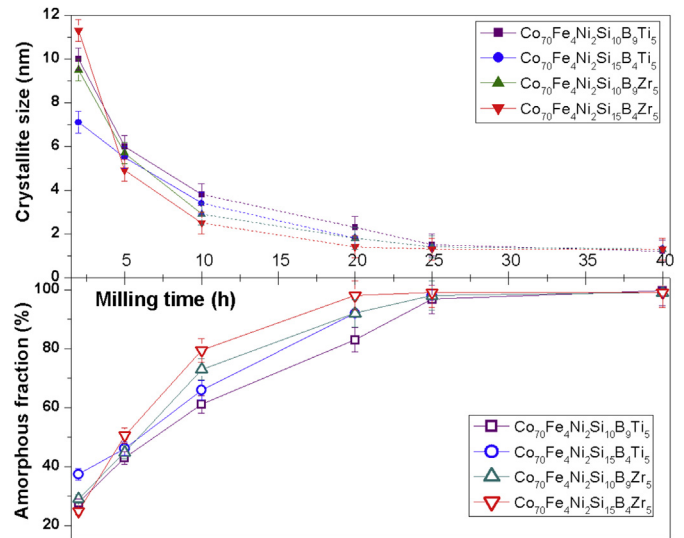


Fig. 2. The evolution of the mean crystallite size and of the amorphous fraction versus milling time for the $\text{Co}_{70}\text{Fe}_4\text{Ni}_2\text{Si}_{15}\text{B}_4\text{Zr}_5$, $\text{Co}_{70}\text{Fe}_4\text{Ni}_2\text{Si}_{15}\text{B}_4\text{Ti}_5$, $\text{Co}_{70}\text{Fe}_4\text{Ni}_2\text{Si}_{10}\text{B}_9\text{Zr}_5$ and $\text{Co}_{70}\text{Fe}_4\text{Ni}_2\text{Si}_{10}\text{B}_9\text{Ti}_5$ alloys.

After 10 h of milling, when the powder consists in an fcc Co-based solid solution, it can be observed that substitution of Zr for either Si or B leads to a slightly lower value of the mean crystallite size as compared to the alloys that contain Ti. This small difference is probably caused by the amount of lattice strain induced by Zr or Ti. The atomic radius of Zr is larger as compared to Ti, resulting in a more stressed lattice which leads to a more brittle material. Increasing the milling time, up to 25 h, leads to quasi-equal values of the mean crystallite size of the prepared alloys regardless of the substitution. For such a long milling duration, our assumption is that the stresses induced by cold working of the material are the main factor which determines the value of the mean crystallite size. In the milling interval 25 h–40 h, almost no variation of the mean crystallite size can be observed for either of the prepared alloys. The saturation of the mean crystallite size vs. milling time is a classic behaviour that has been reported for other alloys obtained by mechanical alloying [24,25].

In Fig. 2 is presented also the evolution of the fraction of amorphous phase in the synthesised alloys as a function of milling time. The introduction of Zr atoms in the material leads to a more pronounced growth of the amount of amorphous fraction upon increasing the milling time as compared to the Ti atoms for both type of substituted atoms, Si and B. This behaviour is also related to the atomic radius of the atoms that have been introduced in the material, which is larger as compared to the atomic radius of the substituted atoms (Si or B). This most probably leads to a higher degree of structural disorder and a large number of structural defects in the material, favouring thus the increase of the amount of amorphous phase. Increasing the milling time from 25 h up to 40 h is not leading to any significant variation of the volume occupied by the amorphous fraction. A similar behaviour can be observed for the variation for the mean crystallite size. After 40 h of milling, regardless of the substitution, the volume occupied by the amorphous phase reaches 99%.

The chemical composition of the amorphous samples (wet milled up to 40 h) is given in Table 1.

Due to the fact that light elements, such as Be, B, C, N, O and F, are generally difficult or impossible to be correctly quantified by EDX technique, the chemical composition of the sample appear to be modified. Thus, the amount of Fe detected is higher than the

Table 1

Chemical composition of the amorphous samples (wet milled up to 40 h) determined by EDX analysis. The given values are given in at%.

	$\text{Co}_{70}\text{Fe}_4\text{Ni}_2\text{Si}_{15}\text{B}_9$	$\text{Co}_{70}\text{Fe}_4\text{Ni}_2\text{Si}_{15}\text{B}_4\text{Zr}_5$	$\text{Co}_{70}\text{Fe}_4\text{Ni}_2\text{Si}_{15}\text{B}_4\text{Ti}_5$	$\text{Co}_{70}\text{Fe}_4\text{Ni}_2\text{Si}_{10}\text{B}_9\text{Zr}_5$	$\text{Co}_{70}\text{Fe}_4\text{Ni}_2\text{Si}_{10}\text{B}_9\text{Ti}_5$
Co	77.6	71.7	73.79	75.67	76.64
Fe	5.4	7.7	5.86	7.27	6.75
Ni	2.1	2.04	2.31	2.51	1.99
Si	14.9	14.29	13.38	9.66	9.66
B	-	-	-	-	-
Zr	—	4.23	—	4.89	—
Ti	—	—	4.7	—	4.96

theoretical one. This is a common effect of processing materials through mechanosynthesis and is assumed that a contamination with 1–4 wt.% Fe is normally expected. This is given by the wearing and tearing of the milling bodies (made from steel) and the assimilation of these impurities into the processed powder [4].

The thermal stability of the amorphous alloys was investigated by DSC measurements under high purity argon atmosphere. The DSC curves of the amorphous alloys are presented in Fig. 3. It can be observed that all curves reveal an exothermic peak in the temperature range 120–300 °C. Due to the nature of mechanosynthesis technique (the particles are subjected to severe cold plastic deformation) a large amount of structural stresses and defects are induced in particles. The above mentioned exothermic peak is related to the release of the internal stresses induced by mechanical alloying process. In the temperature range 440–535 °C the onset of a large exothermic reaction (exothermic peak) can be remarked. This exothermic peak was attributed to the primary crystallisation of the amorphous samples. It can be observed that the crystallisation temperature (the onset) is dependent on the chemical composition of the samples. Comparing the crystallisation temperature of the reference alloy with crystallisation temperature of the alloys obtained by substitution of 5 at.% of Ti or Zr for Si or B the following can be observed:

(i) The substitution of 5 at.% of Zr or Ti for B leads to a small increase of the crystallisation onset from 442 °C

(corresponding to reference sample) to 448 °C and 456 °C for $\text{Co}_{70}\text{Fe}_4\text{Ni}_2\text{Si}_{15}\text{B}_4\text{Zr}_5$ and $\text{Co}_{70}\text{Fe}_4\text{Ni}_2\text{Si}_{15}\text{B}_4\text{Ti}_5$ compositions respectively.

(ii) The substitution of 5 at.% of Zr or Ti for Si leads to a significant increase of the thermal stability of the amorphous alloys with 18%–21% respectively. The crystallisation onset increase from 442 °C (corresponding to reference sample) to 522 °C and 534 °C for $\text{Co}_{70}\text{Fe}_4\text{Ni}_2\text{Si}_{10}\text{B}_9\text{Zr}_5$ and $\text{Co}_{70}\text{Fe}_4\text{Ni}_2\text{Si}_{10}\text{B}_9\text{Ti}_5$ compositions respectively.

The enhancement of the thermal stability of the amorphous phase observed for the alloys in which 5 at.% of Zr or Ti was substituted for Si can be related to the so called geometrical effects. The addition of atoms with different atomic radii will probably leads to a more dense random packed structure. In such a structure, the atomic diffusion (needed for sample crystallisation) is slowed down, stabilising thus the amorphous phase. A detailed study that presents the influence of additions on the crystallisation temperature of Fe-based amorphous alloys is presented in Refs. [26,27]. It was shown that the addition of large atoms leads to increased viscosity of the alloy and increased crystallization temperature. Our present results are in agreement with such an interpretation.

According to the XRD investigations presented in Fig. 4, the primary crystallisation of the samples (all substitution alloys) leads to the formation of the following phases: an fcc Co-based solid solution and Co_2Si . Around temperature of 670 °C, an endothermic reaction can be noticed in the DSC curve. This was attributed to the Curie temperature of one of the crystalline phases obtained from

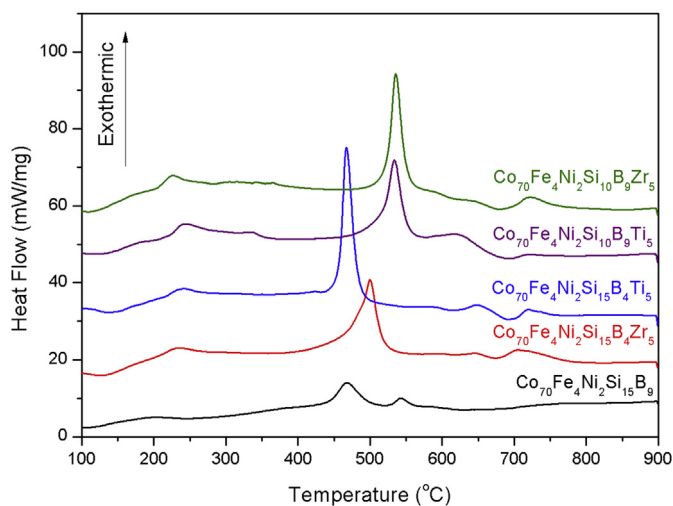


Fig. 3. DSC curves of the amorphous reference alloy ($\text{Co}_{70}\text{Fe}_4\text{Ni}_2\text{Si}_{15}\text{B}_9$) comparison to that recorded for $\text{Co}_{70}\text{Fe}_4\text{Ni}_2\text{Si}_{15}\text{B}_4\text{Zr}_5$, $\text{Co}_{70}\text{Fe}_4\text{Ni}_2\text{Si}_{15}\text{B}_4\text{Ti}_5$, $\text{Co}_{70}\text{Fe}_4\text{Ni}_2\text{Si}_{10}\text{B}_9\text{Zr}_5$ and $\text{Co}_{70}\text{Fe}_4\text{Ni}_2\text{Si}_{10}\text{B}_9\text{Ti}_5$ samples. The DSC curves correspond to the amorphous samples, wet milled up to 40 h. For clarity reasons the curves were vertically shifted.

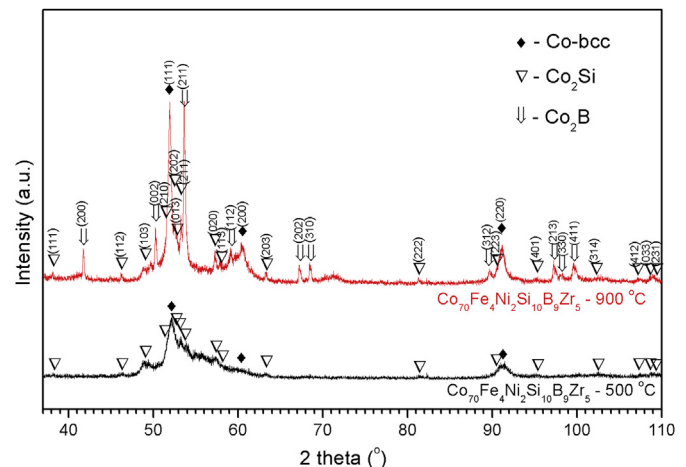


Fig. 4. Room temperature X-ray diffraction patterns of the $\text{Co}_{70}\text{Fe}_4\text{Ni}_2\text{Si}_{10}\text{B}_9\text{Zr}_5$ amorphous alloy obtained after 40 h of wet mechanical milling and subsequent DSC analysis at 500 °C and 900 °C.

primary crystallisation of the amorphous phase. Considering that the Co_2Si phase is paramagnetic at temperatures that exceed $-110\text{ }^\circ\text{C}$ [28], we attribute this Curie temperature to the fcc Co-based solid solution. At $720\text{ }^\circ\text{C}$ a small exothermic reaction can be noticed. This reaction was attributed to the crystallisation of the remaining boron rich amorphous matrix. This event is also encountered on the DSC curve of the reference sample and takes place around $550\text{ }^\circ\text{C}$. The higher temperature of the secondary crystallisation event, noticed for the alloys containing Zr or Ti, can be induced by the larger atoms that are present also in the remaining amorphous matrix, enhancing thus its thermal stability. This supposition is confirmed by the fact that the XRD patterns of the samples heated up to $900\text{ }^\circ\text{C}$ reveal the formation, beside the Co-based solid solution and Co_2Si phases, of the Co_2B phase. The former 2 events are better visible on the DSC curves of the alloys in which Si or B were partially replaced by Zr or Ti.

In order to determine the Curie temperature (T_C) of the amorphous alloys, thermomagnetic measurements were performed. The thermomagnetic curves corresponding to the reference alloy ($\text{Co}_{70}\text{Fe}_4\text{Ni}_2\text{Si}_{15}\text{B}_9$) and $\text{Co}_{70}\text{Fe}_4\text{Ni}_2\text{Si}_{15}\text{B}_4\text{Zr}_5$, $\text{Co}_{70}\text{Fe}_4\text{Ni}_2\text{Si}_{15}\text{B}_4\text{Ti}_5$, and $\text{Co}_{70}\text{Fe}_4\text{Ni}_2\text{Si}_{10}\text{B}_9\text{Zr}_5$ are presented in Fig. 5. The Curie temperature of the alloys was considered to be the temperature at which the magnetisation deviates from linearity in the temperature range where magnetisation strongly decreases. The Curie temperature of the reference sample in amorphous state is $161\text{ }^\circ\text{C}$. It can be observed that substitution of 5 at.% of either Zr or Ti for either B or Si leads to an increased T_C of the alloys by about $100\text{ }^\circ\text{C}$. The largest T_C among the investigated alloys ($287\text{ }^\circ\text{C}$) was observed for the alloy in which 5 at.% of Si was replaced by the same amount of Zr. The observed increase of the Curie temperature as compared to the reference alloy can be explained by a stronger magnetic interaction between magnetic atoms contained in the alloys. Introducing large atoms such as Zr or Ti can lead to significant changes in the compositional short range order of the alloys, which influences the magnetic exchange interaction. Indeed, the increase of the interatomic distances in the alloy is inducing a reinforcement of the exchange interactions between 3 d atoms as expected from the Slater-Neel curve [29].

Above about $450\text{ }^\circ\text{C}$, the increase of the temperature leads to an augmentation of the sample's magnetisation of the suggesting a change of phases and in particular their crystallisation, as expected from the above discussed DSC results. According to XRD

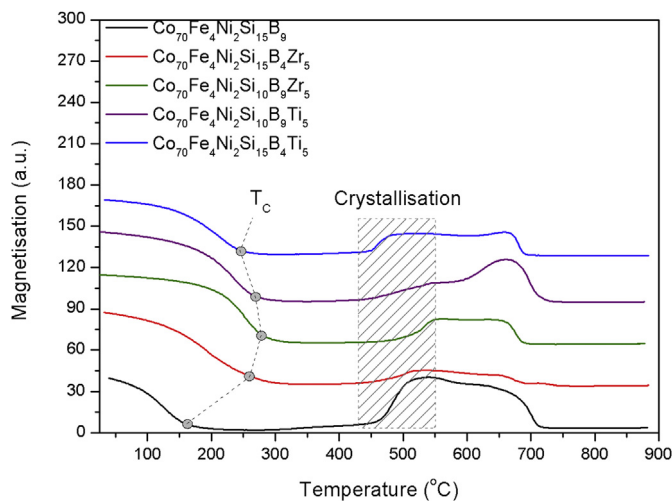


Fig. 5. Thermomagnetic curves corresponding to the amorphous reference alloy ($\text{Co}_{70}\text{Fe}_4\text{Ni}_2\text{Si}_{15}\text{B}_9$) and $\text{Co}_{70}\text{Fe}_4\text{Ni}_2\text{Si}_{15}\text{B}_4\text{Zr}_5$, $\text{Co}_{70}\text{Fe}_4\text{Ni}_2\text{Si}_{15}\text{B}_4\text{Ti}_5$, and $\text{Co}_{70}\text{Fe}_4\text{Ni}_2\text{Si}_{10}\text{B}_9\text{Zr}_5$. For clarity reasons the curves were vertically shifted.

investigations, the only phase that is ferromagnetic at this temperature (for the investigated alloys) is the fcc Co-based solid solution. The T_C of this phase determined from the $M(T)$ curves is around $700\text{ }^\circ\text{C}$ which is different as compared to the one determined from DSC curves ($670\text{ }^\circ\text{C}$). The different values of the T_C derived from DSC and thermomagnetic measurements can be explained by the different heating rates and different investigation techniques which record different signal given by the sample.

Fig. 6 presents the milling time dependence of the saturation magnetisation for the as-milled alloys. For comparison reasons, the saturation magnetisation of the starting sample of each alloy is presented as well as the value of the saturation magnetisation of the reference alloy. The values of saturation magnetisation have been derived from the first magnetisation curves measured up to 10 T by extrapolation to zero field of the magnetization obtained in the magnetic field higher than 4 T. It can be observed that the saturation magnetisation decreases upon increasing milling time for all the studied alloys. The saturation magnetisation of the new alloys formed by milling has, as expected, a lower value as compared to the one of the starting sample, because of the nonmagnetic elements which are progressively alloyed in the cobalt structure.

In the first hours of milling, the decrease of the saturation magnetisation can be related to the dissolution of nonmagnetic atoms into the structure of 3 d magnetic atoms (mainly cobalt). During formation of the alloy the metalloids, such as B and Si, are chemically bonding with the ferromagnetic atoms Co (also Fe and Ni), effect that induces a reduction of their magnetic moments [30–32] as a result of the (Co, Fe) 3 d – p (Si, B) electronic hybridization. Further decrease of the saturation magnetisation upon increasing milling time up to 40 h can be explained by the large number of structural defects and internal stresses induced by high energy mechanical milling. In addition, it was proved that, a certain decrease of the saturation magnetisation is assumed to be given by the wet milling conditions as follow: (i) a certain amount of PCA is adsorbed on the particles surface; (ii) the PCA decomposition leads to the contamination of the alloys with nonmagnetic atoms (in our case C atoms) [33, 34]. The decrease of the magnetisation can also be linked to the crystalline to amorphous transformation which occurs upon increasing milling time. A decrease of the saturation magnetisation upon increasing milling time was also reported

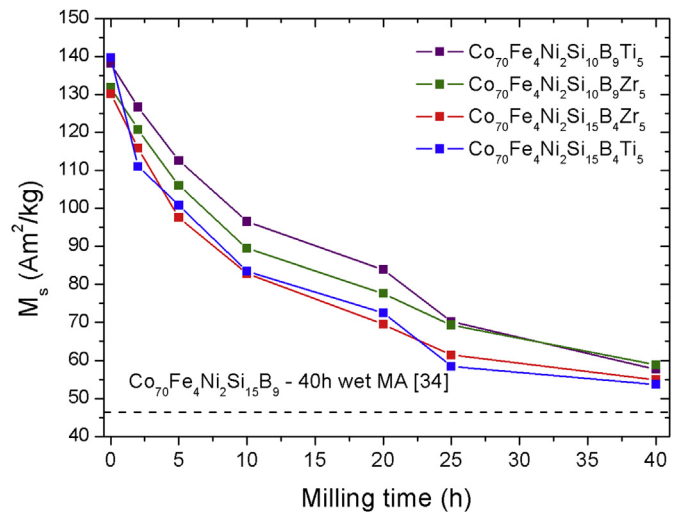


Fig. 6. Evolution of saturation magnetisation upon increasing milling time for the wet mechanically alloyed powders. By dashed line is shown the saturation magnetisation of the reference alloy.

when rapidly solidified $\text{Co}_{70.3}\text{Fe}_{4.7}\text{Si}_{10}\text{B}_{15}$ (at.%) ribbons were subjected to milling in a vibratory ball mill up to 1500 h. The decrease of the sample magnetisation was explained by the presence of a fraction of small particles having a superparamagnetic behaviour [13]. Such a phenomena can also be considered in the case of our study if we take into account that wet mechanical alloying promotes the fracturing phenomena in detriment of cold welding phenomena [4].

It can be observed that the partial substitution of either Ti or Zr for Si or B leads to a saturation magnetisation higher than the one corresponding to reference alloy although the reference alloy was processed in identical conditions. The saturation magnetisation of the sample obtained by wet milling up to 40 h, in which B was partially replaced by Zr or Ti, is 14% larger than that of reference alloy. When Si was partially replaced by Zr or Ti an increase of the saturation magnetisation by about 20% can be remarked. This clearly shows that metalloid atoms are more efficient to reduce the magnetization of the (Fe, Co, Ni) majority elements than Zr or Ti.

The calculation of the average magnetic moment per 3 d atom (Co, Fe, Ni) reveal the following values for the amorphous samples wet milled up to 40 h:

- For the reference alloy $\text{Co}_{70}\text{Fe}_4\text{Ni}_2\text{Si}_{15}\text{B}_9$: 0.54 μ_B /alloy atom;
- For $\text{Co}_{70}\text{Fe}_4\text{Ni}_2\text{Si}_{10}\text{B}_9\text{Ti}_5$ alloy: 0.68 μ_B /atom
- For $\text{Co}_{70}\text{Fe}_4\text{Ni}_2\text{Si}_{10}\text{B}_9\text{Zr}_5$ alloy: 0.74 μ_B /atom
- For $\text{Co}_{70}\text{Fe}_4\text{Ni}_2\text{Si}_{15}\text{B}_4\text{Ti}_5$ alloy: 0.66 μ_B /atom
- For $\text{Co}_{70}\text{Fe}_4\text{Ni}_2\text{Si}_{15}\text{B}_4\text{Zr}_5$ alloy: 0.7 μ_B /atom

It was proved that Co or Fe bonds strongly to all metalloid atoms like B or Si resulting in a reduction of its magnetic moment. The diminution of d states of Co with p states of metalloid atoms in which the hybridised orbitals are non-magnetic [35]. According to this, the replacement of metalloids atoms (Si or B) by other transitional metals (in our case Zr or Ti) will lead to larger value of magnetic moment of cobalt. As a consequence, the saturation magnetisation of the alloys is larger than the one corresponding to the reference sample.

4. Conclusions

Starting from a mixture of elemental powders corresponding to the stoichiometric composition of $\text{Co}_{70}\text{Fe}_4\text{Ni}_2\text{Si}_{15}\text{B}_9$ (at.%), an amorphous alloy (reference alloy) was prepared by wet mechanical alloying. In order to determine the influence of either the substituted element, or the substitution element, deriving from this composition, 4 alloys were synthesized by 5 at.% substitution of transition metals (Ti or Zr) for metalloids (Si or B). After the investigation of the amorphous alloys obtained by mechanical alloying, the following conclusions can be drawn:

- Regardless of the substitution or substituted element the milling duration needed for alloy amorphisation is 40 h, which is identical to the one corresponding to the reference alloy.
- Upon increasing milling time a continuous decrease of the mean crystallite size was observed and, as a consequence, an increase of the volume occupied by the amorphous fraction is remarked.
- The DSC investigations revealed that the substitution of Ti or Zr for B has low influence over the crystallisation temperature of the amorphous phase. Meanwhile, the substitution of Zr or Ti for Si leads to an increase of the crystallisation temperature of the alloys by 18% and 21% respectively. This indicates a larger stability range of the amorphous phase.

- Thermomagnetic measurements evidenced a substantial increase of the Curie temperature of the substituted alloys as compared to the reference sample. The largest T_C (287 °C) was observed for the alloy in which Si was replaced by Zr.
- It was pointed out that the partial substitution of either Ti or Zr for Si or B leads to a saturation magnetisation higher than that of the reference alloy by 14%–20%.

Whereas both transition metals (Ti and Zr) and metalloids (Si and B) are nonmagnetic elements and play in favour of a dilution of the magnetization of the other elements like Fe, Co or Ni, the presence of B or Si is much more efficient to reduce the magnetization of the alloy as a result of the 3 d (Co,Fe,Ni) states hybridization with the p states of metalloids.

Acknowledgements

This work was supported by a Grant of the Romanian National Authority for Scientific Research CNCS – UEFISCDI, Project number PN II-RU-TE-2012-3-0367.

References

- [1] P. Duwez, *Trans. Am. Soc. Met.* 60 (1967) 607–633.
- [2] G. Herzer, *Acta Mater.* 61 (2013) 718–734.
- [3] C. Suryanarayana, A. Inoue, *Bulk Metallic Glasses*, CRC Press, 2010, pp. 145–186.
- [4] C. Suryanarayana, *Prog. Mater. Sci.* 46 (2001) 1–184.
- [5] E. Gaffet, G. Le Caër, *Mechanical processing for nanomaterials*, in: H.S. Nalwa (Ed.), *Encyclopedia of Nanoscience and Nanotechnology*, 2004, pp. 1–39.
- [6] E. Gaffet, *Mater. sci. Eng. A* 132 (1991) 181–193.
- [7] C.C. Koch, J.D. Whittenberger, *Intermetallics* 4 (1996) 339–355.
- [8] M.E. McHenry, M.A. Willard, D.E. Laughlin, *Prog. Mater. Sci.* 44 (1999) 291–433.
- [9] M. Xueming, Y. Lanping, D. Yuanda, *Chin. Phys. Lett.* 8 (1991) 436–438.
- [10] L.M. Kubalova, V.I. Fadeeva, I.A. Sviridov, *Rev. Adv. Mater. Sci.* 18 (2008) 360–365.
- [11] M. Peškaia, M. Jachimowicz, V.I. Fadeeva, H. Matyja, *J. Non Cryst. Solids* 287 (2001) 360–365.
- [12] A.M. Bolarín-Miró, F. Sánchez-De Jesús, G. Torres-Villaseñor, C.A. Cortés-Escobedo, J.A. Betancourt-Cantera, *J. Non Cryst. Solids* 357 (2011) 1705–1709.
- [13] J. Bednarcík, J. Kováč, P. Kollár, S. Roth, P. Sovák, J. Balcerski, K. Polanski, T. Svec, *J. Non Cryst. Solids* 337 (2004) 42–47.
- [14] A.H. Taghvaei, M. Stoica, M.S. Khoshkhou, J. Thomas, G. Vaughan, K. Janghorban, J. Eckert, *Mater. Chem. Phys.* 143 (2012) 1214–1224.
- [15] H.M. Wu, C.J. Hu, H.C. Li, *J. Alloys Comp.* 483 (2009) 553–556.
- [16] L.M. Moreno, J.S. Blázquez, J.J. Ipus, A. Conde, *J. Alloys Comp.* 585 (2014) 485–490.
- [17] J. Fúzer, J. Bednarcík, P. Kollár, S. Roth, *J. Magn. Magn. Mater.* 310 (2007) e852–e854.
- [18] P. Kollár, J. Bednarcík, S. Roth, H. Grahl, J. Eckert, *J. Magn. Magn. Mater.* 278 (2004) 373–378.
- [19] P. Scherrer, *Mathematisches Physikalische Kl I* (1918) 98–100.
- [20] J.M. Grenèche, A. Lawska-Waniewska, *J. Magn. Magn. Mater.* 264 (2000) 215–216.
- [21] H.W. Song, S.R. Guo, Z.Q. Hu, *Nanostruct. Mater.* 11 (1999) 203–210.
- [22] J.Y. Huang, Y.K. Wu, H.Q. Ye, *Acta Mater.* 44 (1996) 1201–1209.
- [23] B. Avar, S. Ozcan, *J. Alloys Compd.* 650 (2015) 53–58.
- [24] H. Moumeni, S. Alleg, J.M. Grenèche, *J. Alloys Compd.* 419 (2006) 140–144.
- [25] B.V. Neamtu, I. Chicinaş, F. Popa, V. Pop, *Intermetallics* 19 (2011) 19–25.
- [26] J.L. Walter, *Mater. Sci. Eng.* 50 (1981) 137–142.
- [27] B.V. Neamtu, H.F. Chicinaş, T.F. Marinca, O. Isnard, I. Chicinaş, *Adv. Powder Technol.*, under review.
- [28] G. Liu, Y.C. Lin, L. Liao, L. Liu, Y. Chen, Y. Liu, N.O. Weiss, H. Zhou, Y. Huang, X. Duan, *Nano. Lett.* 12 (2012) 1972–1976.
- [29] L. Néel, *Ann. Phys. Paris.* 5 (1936) 232–279.
- [30] B.W. Corb, R.C. O’Handley, N.J. Grant, *Phys. Rev. B* 27 (1983) 636–641.
- [31] C. Chacon, O. Isnard, *J. Appl. Phys.* 89 (2001) 71–75.
- [32] O. Isnard, D. Fruchart, *J. Alloys Comp.* 205 (1994) 1–15.
- [33] B.V. Neamtu, O. Isnard, I. Chicinas, C. Vagner, N. Jumate, P. Plaindoux, *Mater. Chem. Phys.* 125 (2011) 364–369.
- [34] B.V. Neamtu, T.F. Marinca, I. Chicinaş, O. Isnard, F. Popa, *Adv. Powder Technol.* 26 (2015) 323–328.
- [35] B.W. Corb, R.C. O’Handley, N.J. Grant, *J. Appl. Phys.* 53 (1982) 7728–7730.